5-2014

Fluorescence Imaging of Microdialysis Sampling

Jordan Leigh Haynie
University of Arkansas, Fayetteville

This thesis is approved.

Thesis Advisor:

Dr. Julie Stenken

Thesis Committee:

Dr. Robert Beitle

Dr. Ed Clausen

Fluorescence Imaging of Microdialysis Sampling

An Undergraduate Honors College Thesis

in the

Department of Chemical Engineering
College of Engineering
University of Arkansas
Fayetteville, AR

by

Jordan Leigh Haynie

April 21, 2014

Acknowledgments

I would like to thank Dr. Julie Stenken for all of her time, support, and guidance throughout my research project. I would like to thank Cynthia Sides and the rest of Dr. Stenken's lab group for all of their patience and advice. I would also like to thank Dr. Robert Beitle and Dr. Ed Clausen for taking the time to serve on my thesis committee.

Abstract

Many biomolecules including proteolytic enzymes known as matrix metalloproteinases (MMPs) are released when a material, such as a microdialysis probe, is implanted in a living organism. The MMPs cleave structural protein components of the extracellular matrix and play an important role in biological functions such as wound healing.[1-3] Many enzymatic substrates for MMPs have fluorescent product mimics, and the mimics can be used as agents to monitor biochemical processes.[1]

In this study, microdialysis, a minimally invasive sampling technique, was combined with fluorescence imaging to determine the possibility of monitoring microdialysis in real-time, and thus provide a method that could ultimately lead to the ability to monitor localized MMPs.. *In vitro* studies were conducted with fluorescent dyes IR-820 and Rhodamine B, producing promising results that illustrate combining microdialysis and fluorescence imaging is quite feasible. The IR-820 was unpredictable during *in vitro* studies; therefore, it was not used *in vivo*, and Rhodamine B was selected to develop and optimize the combined method due to its stability. Microdialysis probes embedded in agarose phantoms, perfused with Rhodamine B, and imaged via a fluorescent imaging system clearly revealed a diffusion profile developing with time. Increased intensity surrounding the probe during infusion was also visible.

1. Objectives

The objective of this project is to determine the feasibility of combining *in vivo* fluorescence imaging with microdialysis sampling. Specifications to consider for this coupled method include the sensitivity of the imaging method, the distance the dye can be imaged from the microdialysis probe during long-term infusion, and the ability of the instrument to monitor a time-course during infusion. These conditions are affected by extraction properties of microdialysis sampling, such as analyte diffusion coefficients and kinetic rate constants. However, these parameters are poorly characterized in the tissue space.[4] *In vivo* fluorescence imaging of diffusion profiles resulting from infused near-infrared (NIR) dyes through an implanted microdialysis probe provides a real-time and uniquely innovative approach toward visually observing mass transport processes affecting microdialysis sampling extraction efficiency. Interpreting *in vivo* data from the combined methods of fluorescence imaging and microdialysis sampling first requires a thorough understanding of the process *in vitro*.

In vitro models are often used to model biological process. Phantoms are imaging models of known geometric dimensions and material construction. They are most often used in research of medical imaging to provide a tissue-like material for *in vitro* studies.[5] Microdialysis probes embedded in phantoms, perfused with fluorescent dye, and imaged can reveal whether or not a diffusion profile can be detected.

A long term goal of this project is to determine if localized matrix metalloproteinases (MMPs) can be measured via this coupled method of live imaging of microdialysis. When a material, such as a microdialysis probe, is implanted in a living organism, a foreign body reaction (FBR) occurs, leading to the release of many biomolecules including proteolytic enzymes known as MMPs, which cleave structural protein components of the extracellular

matrix and play an important role in pathogenic and biological functions such as wound healing.[1-3] Many enzymatic substrates for MMPs have fluorescent product mimics, such as elastase, which displays substrate specificity similar to MMP-12, and can therefore be used as agents to monitor biochemical processes.[1]

2. Background

2.1 Microdialysis Sampling

In vivo microdialysis sampling is a widely-used, minimally-invasive sampling technique. A perfusion fluid is infused at μL/min flow rates through the lumen of a hollow-fiber dialysis membrane, allowing delivery of a solution and collection of unbound solutes from extracellular fluid (Figure 1).[6,7] The resulting dialysate represents the biochemical functions of molecules surrounding the dialysis probe. Parameters influencing extraction properties such as diffusion coefficients and kinetic rate constants are difficult to know *a priori*. Few methods allow researchers to peek into what is happening within a biological system; one of these methods is *in vivo* fluorescence imaging.

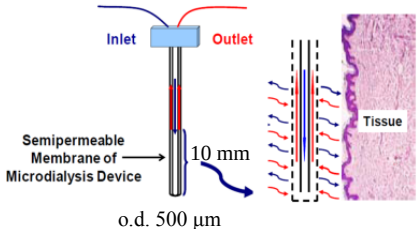

Figure 1. Diffusion across a microdialysis probe.

Relative recovery relates the concentration of a substance in the extracellular fluid and the concentration of the same substance in the dialysate; it is the concentration of the substance in the dialysate divided by its concentration in the extracellular fluid shown in Equation 1

$$R = \frac{C_{in} - C_{dial}}{C_{in}} \qquad \text{Equation 1}$$

where C_{in} and C_{dial} are the perfusate and dialysate concentrations of a compound, respectively.[8] There are several variables that influence the relative recovery of a system. The relative recovery is inversely proportional to the flow rate, with commonly used flow rates ranging from 0.1 μL/min to 5 μL/min. Recovery will increase linearly with an increase in membrane surface area when a high concentration gradient is maintained between extracellular fluid and the dialysate. At higher temperatures diffusion increases, thus recovery increases at higher temperatures. Other variables that affect relative recovery include membrane and tubing material and geometry and perfusate composition.[8]

During microdialysis sampling, there are three regions of mass flux: the dialysate, the membrane, and the bulk solution (*in vitro*) or the tissue (*in vivo*). The following equations describe the flux occurring in each region.[9] For simplification, Cartesian coordinates are used (Figure 2), noting the true model requires the use of cylindrical coordinates.

$$j_{dialysate} = -D_{dialysate}\frac{dc}{dx} \quad (1)$$

$$j_{membrane} = -D_{membrane}\frac{dc}{dx} \quad (2)$$

$$j_{bulk\ solution} = -D_{bulk\ solution}\frac{dc}{dx} \quad (3)$$

$$j_{tissue} = -D_{tissue}\frac{dc}{dx} - k[c] \quad (4)$$

In these equations, *j* is the flux, *D* is the diffusion coefficient, *c* is the concentration of the solute, and *x* is the position within the system. For tissue, the flux must take kinetic removal processes into account.[9] The flux in tissue is described by Equation 4, where *k* is a lumped kinetic removal term that includes removal via capillary permeability and metabolism.

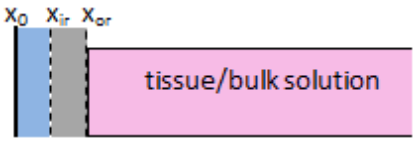

Figure 2. The dialysate, dialysis probe membrane and tissue/bulk solution. x_0 to x_{ir} : dialysate. x_{ir} to x_{or}: probe

2.2 Coupling Microdialysis Sampling with Fluorescence Imaging

During fluorescence imaging, a fluorescent dye is subject to a certain wavelength of light that excites electrons. Electrons then relax, emitting a photon at a wavelength related to the energy difference between the excited and relaxed states.[10] Through imaging the fluorescence *in vivo*, the "visualization of biology in its intact and native physiological state" is possible. [10, 11]

By utilizing *in vivo* fluorescence imaging of microdialysis, the real-time occurrence of the diffusion process between introducing the perfusion fluid to the system and collecting the dialysate can be viewed by creating appropriate mathematical models of diffusion and kinetics for microdialysis sampling and correlating experimental microdialysis data *in vitro*.

The imaging system used in this study is an IVIS Lumina *XR*. The IVIS system is equipped with a charge coupled device (CCD) that has a spatial resolution of 1024x1024 pixels.[12] The CCD, a photosensitive detector, measures the electrical charge of each pixel in an image and assigns a numerical value to that charge called counts. The electrical charge of each pixel is directly proportional to the amount of light it was exposed to, and the CCD camera saturation is about 60,000 counts.

Several parameters of the IVIS imaging system affecting sensitivity were varied during optimization of the process. These parameters include the binning, the f/stop, and the exposure time. With increased binning, the data for adjacent pixels are combined into bigger and fewer pixels.[13] This allows better signal-to-noise ratio and improves readout speeds. In the IVIS there are binning settings of 1, 2, and 3 (small, medium, high).[12] A binning of 1 has an area of 4x4 pixels, a binning of 2 has an area of 2x2 pixels which gives a signal that is four times that of the 1 binning and is double the spatial size. At a binning of 4 there is a single megapixel with sixteen times the signal and four times the spatial size. As binning increases, the spatial

resolution decreases. However, this can be overcome by decreasing the field of view (FOV, increasing magnification) as the binning is increased, because CCD pixels are smaller at higher levels of magnification.

The IVIS system has f/stop settings ranging from 2 to 16.[12] The f/stop affects the amount of light that is allowed into the camera with lower f/stops allowing more light into the camera. Lower f/stops decrease the depth of the field imaged, but contain increased sensitivity. Exposure time also affects sensitivity.[12] Increased exposure time allows increased sensitivity, but needs to be low enough that the image doesn't become saturated and high enough to avoid background "noise".

Radiant efficiency is the suggested measurement for fluorescence, and it is defined as "a fluorescence emission radiance per incident excitation power."[12] The minimum detectable radiance, the photon emission from the subject, for the IVIS is 100 photons/s/sr/cm^2.[12, 14]

3. Materials and Methods

3.1 Chemicals

Rhodamine B, Dextran-500, and Tris(hydroxymethyl)aminomethane (TRIS base), Ethlyenediaminetetraacetic acid (EDTA) were purchased from Sigma-Aldrich (St. Louis, MO). Solutions used in this work were Ringer's solution (147 mM NaCl, 4.6 mM KCl, 2.3 mM $CaCl_2$, pH 7.4); Ringer's and 6% Dextran-500 (pH 7.4); or Ringer's, 6% Dextran-500, and 0.1% (w/v) Bovine Serum Albumin, BSA (Rockland Inc., Gilbertsville, PA), pH 7.4. Agar PCR Plus (EMD Millipore, (San Diego, CA) was used to prepare 2% agar phantoms in a 1:50 diluted Tris-acetate-Ethylenediaminetetraacetic acid (TAE) buffer consisting of 2 M (TRIS base), 7.15 mL

acetic acid, 12.5 mL (EDTA) (0.5 M, pH 8.0), and 62.5 mL HPLC-grade water (Fisher Scientific, Waltham, MA). All other chemicals were reagent grade or better.

3.2 Microdialysis Sampling

CMA-20 microdialysis probes (Harvard Apparatus, (Holliston, MA)) with polyethersulfone (PES) membranes (100 kDa molecular weight cut-off (MWCO) and 10 mm length) were used for all experiments. A BASi microdialysis syringe pump, controller, and syringes (Bioanalytical Systems Inc., West Lafayette, IN, USA) were used to perfuse fluids through the microdialysis probes. For *in vitro* relative recovery experiments, probes were immersed into continuously stirred Rhodamine B solutions (20 μM and 200 μM) in Ringer's heated to 35 °C and perfused with a solution of Ringer's, 6% Dextran-500, and 0.1% (w/v) BSA at 1 μL/min. Samples were collected every hour for five hours. Collected dialysate samples (30 μL to 60 μL) were measured at 556 nm (NanoDrop 2000c, Thermo Scientific, Pittsburgh, Pennsylvania) and concentrations were determined by comparing their absorbance vs. standard curves.

3.3 *In vitro* Imaging

To obtain fluorescence images of dye's diffusion profile, an IVIS Lumina *XR in vivo* imaging system (Caliper Life Sciences, Hopkinton, MA) via Living Image Software (PerkinElmer, Waltham, MA) was used with the following parameters: 5 sec exposure time, small binning, f/stop 2, field of view C, and 535/Cy5.5 excitation/emission filters. Microdialysis probes were embedded in 2% agar phantoms and connected to a CMA pump (CMA, A Harvard Apparatus Company, Holliston, MA) attached to a 12 V battery and perfused at 1 μL/min with

either 20 μM or 200 μM Rhodamine B in a solution of Ringer's, 6% Dextran-500, and 0.1% (w/v) BSA, pH 7.4. Images were obtained at five minute intervals for three hours.

3.4 *In Vivo* Imaging

Background fluorescence images of a naïve male Sprague-Dawley rat (250 g) were obtained at various imaging settings (including the same imaging conditions used for the agar gels as previously described) using the appropriate excitation and emission wavelength filters for Rhodamine B (535 nm, Cy5.5, respectively). Rats were anesthetized in an isoflurane induction chamber and imaged in the Lumina XR while maintaining 2.5% isoflurane/ 0.8 L/min oxygen.

4. Results

Two dyes were used during the experiments for this study: IR-820 and Rhodamine B. IR-820 is a near-infrared (NIR) dye with a molecular weight of 849.47g/mol, and its excitation and emission wavelengths are 710 nm and 820 nm, respectively.[15, 16] Rhodamine B fluoresces in the visible light spectrum. Rhodamine B has a molecular weight of 479.01 g/mol, and the excitation and emission wavelengths are 554 nm and 627 nm, respectively.[17]

4.1 IR-820

Fluorescent dye IR-820 was originally chosen to aid in optimization and method development of combining microdialysis sampling with fluorescent imaging. IR-820 was chosen in part due to the fact that the NIR excitation and emission wavelengths for the dye are suitable for *in vivo* work. However, due to its unpredictable and unexpected behavior witnessed *in vitro*, it was not investigated *in vivo* during this study. *In vitro* IR-820 studies included well plate and

phantom experiments. Figure 3 shows IR-820 in a well plate. This image was taken using the fluorescent imaging settings on the IVIS Lumina *XR* system. The IR-820 was dissolved in water, Ringer's, Ringer's plus Dextran, and Ringer's plus Dextran and BSA to compare its behavior in various solutions. Rows A, C, E, and G contain these solutions, respectively. Wells in column one were filled with a concentration of 235 μM and serial diluted down each row. The strongest fluorescent signal is expected to be in the first column with it weakening as it continues down the row. This is not the case with the IR-820, as seen in the figure below, as it tends to start with a weak or no fluorescent signal, then gradually develops a stronger signal, and finally weakens again.

The IR-820 only strongly fluoresced in water and in Ringer's, 6% Dextran, and 0.1% (w/v) BSA. There is a very small amount of fluorescence in wells E2 thorugh E6 in a solution of Ringer's and 6% Dextran. These wells correlate with with the stronger fluorescent signals in rows A and G which could mean this is an actual fluorescent signal and not simply backgound. Row H contains a solution of Ringer's, 6% Dextran, and 0.1% (w/v) BSA. The signal in this row is thought to be background, and since it is a stronger singal than that in Row E, it could be assumed that the color in Row E is background and not an actual fluorescent signal. As shown in row C, the IR-820 did not fluoresce at all in only Ringer's solution. Note: Rows B, D, F, and H contain water, Ringer's, Ringer's and 6% Dextran, and Ringer's, 6% Dextran, and 0.1% (w/v) BSA, respectively, with no dye. The dye fluoresces much more strongly in Row G, which contains BSA, and Row H shows fluorescence even though there is no dye in the wells. This indicates that BSA may be interefereing with the fluorescent signal of the dye. IR-820 seems to increase in fluorescence intensity with decreasing dye concentration until it reaches a certain

concentration, then the fluorescent intensity decreases with decreasing concenetration. The dye is also not consistent in the way it behaves in the varying solutions shown.

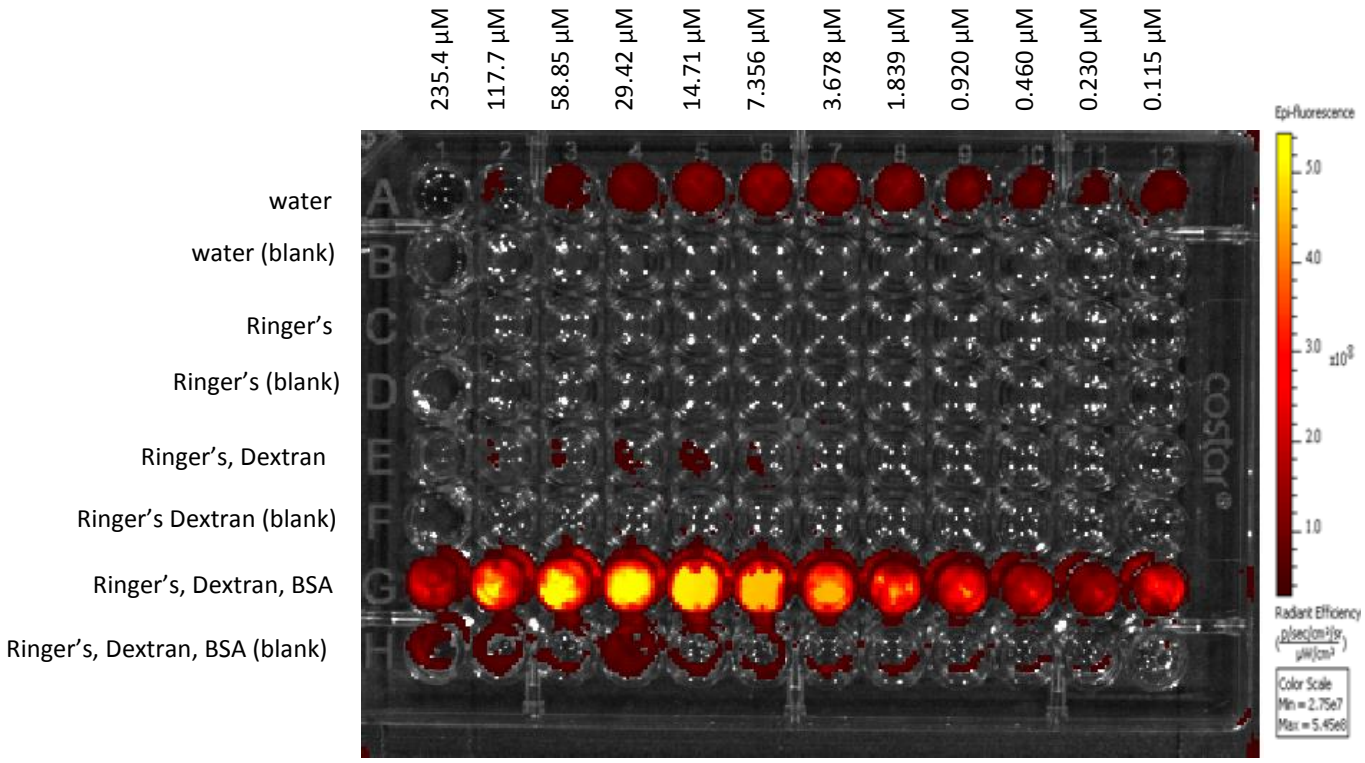

Figure 3. Well plate containing serial diluted IR-820 dye in various solutions. Settings used: medium binning, f/stop 2, and 30 s exposure time.

Instrument Optimization

To determine the optimal imaging settings, parameters of the imaging system were varied to provide an image with the best spatial resolution. A field of view (FOV) of 12.5 cm (FOV D) was used for all plate images, and a FOV of 10 cm (FOV C) was used for phantoms images.

Table 1 displays the methods that were initially used to image IR-820 as it was being perfused through agarose gels. Images were taken of the phantoms every 15 minutes for one hour at each of the methods in the table. Method 002 was no longer applied to IR-820 after this

experiment as there was not any fluorescence detected after 30 minutes of perfusion. Figures 4 and 5 display images for Methods 001 and 005 for IR-820.

Table 1. Methods used to determine imaging settings for IR-820.

Method	Exposure Time (s)	Binning	f/stop	Excitation/Emission Filters
001	0.5	Medium	2	745/ICG
002	1	Small	2	745/ICG
005	60	Small	16	745/ICG

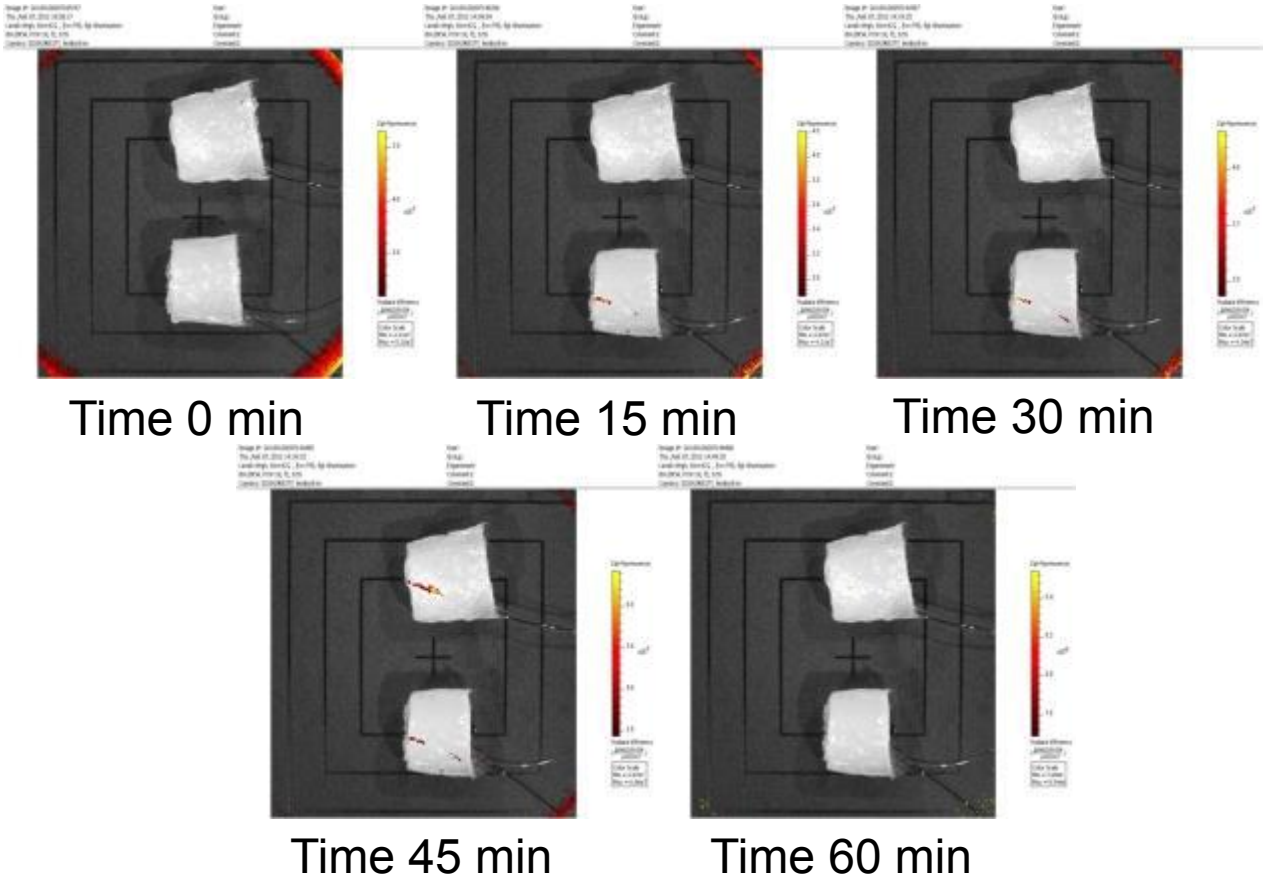

Figure 4. IR-820 dissolved in a solution of Ringer's, 6% Dextran, and 0.1% (w/v) BSA, perfused at 1 µL/min, 0.5 second exposure time, medium binning, f/stop 2, and excitation/emission filters of 745/ICG.

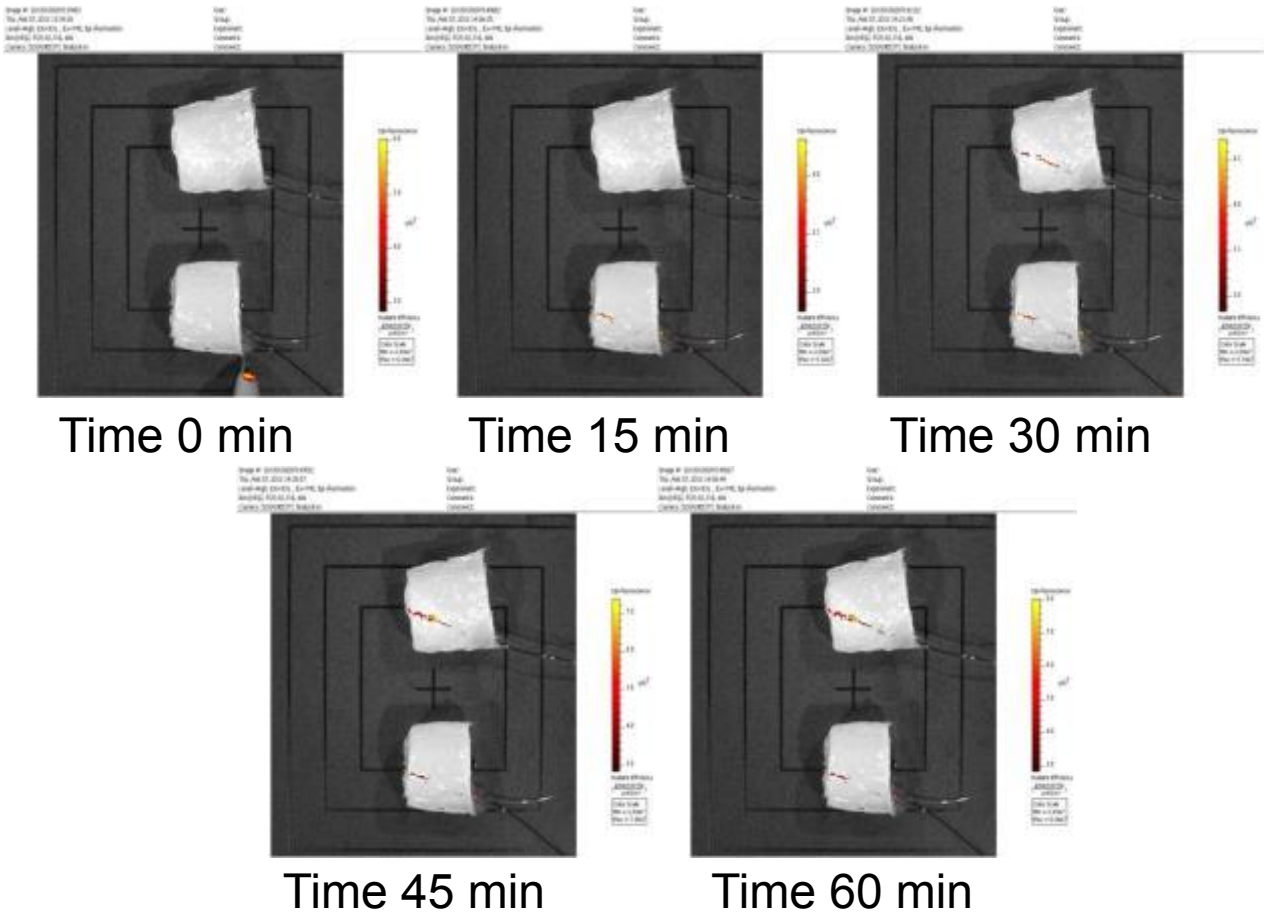

Figure 5. IR-820 dissolved in a solution of Ringer's, 6% Dextran, and 0.1% (w/v) BSA, perfused at 1 μL/min, 60 second exposure time, small binning, f/stop 16, and excitation/emission filters of 745/ICG.

As you can see in Figure 4, the IR-820 is unpredictable. The fluorescence intensity should increase with each 15 minute interval; however, there is no fluorescence detected after 60 minutes of perfusion, even though fluorescence is clearly seen after 45 minutes of perfusion. In Figure 5, an increase in fluorescence intensity is seen from one image to the next. The dye was expected to spread out from the probe, developing a diffusion profile, however the dye appears to remain close to the probe.

4.3 Rhodamine B

Because IR-820 proved unpredictable, fluorescent dye Rhodamine B was chosen for its stability to aid in the development and optimization of this combined method.

Instrument Optimization

Table 2 displays the imaging settings examined for Rhodamine B. Methods 001, 002, and 005 are the same settings used with IR-820, but the excitation and emission filters were changed to suite the excitation and emission characteristics of Rhodamine B.

Table 2. Methods used to determine imaging settings for Rhodamine B.

Method	Exposure Time (s)	Binning	f/stop	Excitation/Emission Filters
001	0.5	Medium	2	535/Cy5.5
002	1	Small	2	535/Cy5.5
003	1	Medium	2	535/Cy5.5
004	1	Small	16	535/Cy5.5
005	60	Small	16	535/Cy5.5
006	1	Small	4	535/Cy5.5
007	1	Small	8	535/Cy5.5

First, the same methods that were applied to IR-820 were applied to Rhodamine B while perfusing it through microdialysis sampling probes implanted in agarose gels. Background images (time at t=0) taken for Methods 001 and 005 returned too much background "noise" meaning the image showed there was fluorescence when there wasn't anything fluorescent in the frame suggesting background scatter or unexpected autofluorescence. Some background fluorescence can be removed by manually scaling the radiant efficiency, but I have found that removing extensive amounts of background "noise" can remove data as well.

The minimum of the scale is determined by the amount of background present in the image at time t=0, or the background image. The background image is manually scaled to subtract any "noise" that may be visible in the image. After most, if not all, of the background is removed from the background image, the minimum on the scale for the background image is

used as the absolute minimum for the remaining images. The minimum may be raised slightly depending on whether or not there seems to be excessive fluorescence around the probe (or if a previously used probe is used again and it still has some dye in it). During the first experiment conducted, new probes were used. The minimum determined during this experiment was the basis for the minimum on following experiments. Figures 6-8 show the steps for this method.

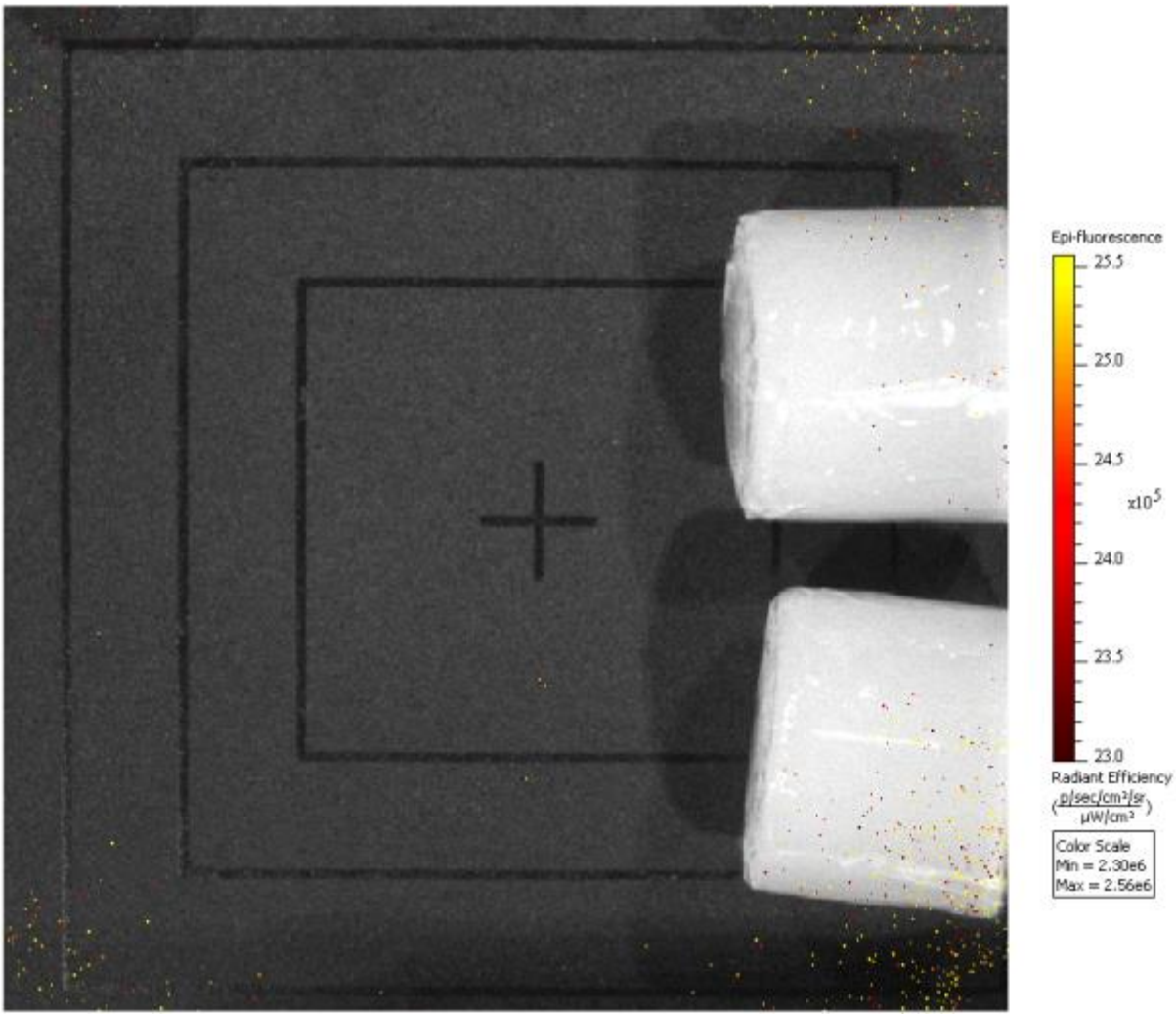

Figure 6. Agar phantoms at time t=0 minutes. Perfusion has not started, but there is background "noise surrounding the frame of the image. Note the minimum on the scale is 2.3×10^6 [(p/sec/cm^2/sr)/(µW/cm^2)].

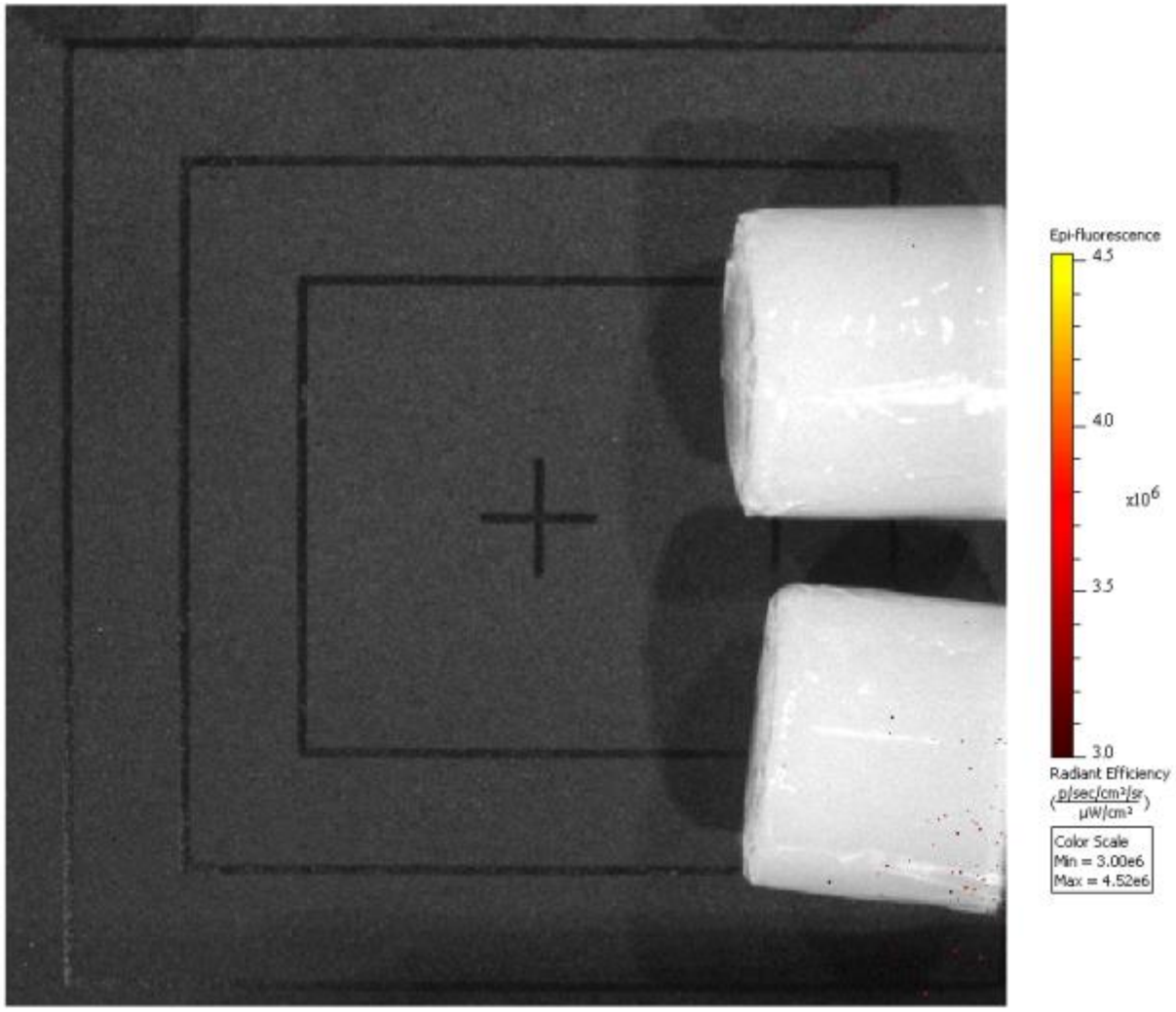

Figure 7. Agar phantoms at time t=0 minutes. Perfusion has not started. There is less background "noise" than in Figure 6. This is because the minimum on the scale was increased to remove background. Note the minimum on the scale is $3x10^6$ [(p/sec/cm^2/sr)/(µW/cm^2)].

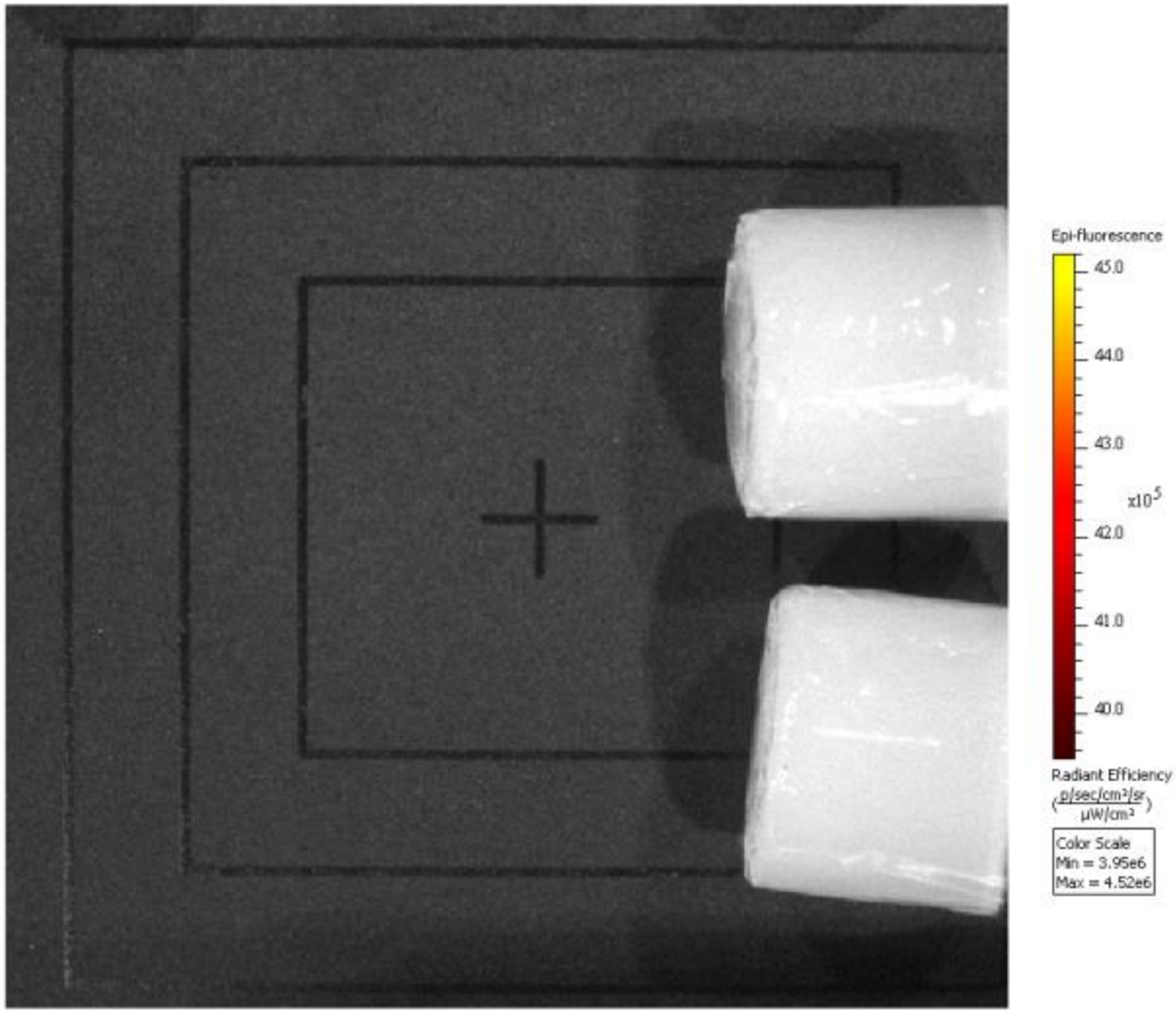

Figure 8. Agar phantoms at time t=0 minutes. Perfusion has not started. Background "noise" has been removed because the minimum on the scale was increased until there wasn't any background in the image. Note the minimum on the scale is 3.95×10^6 [(p/sec/cm^2/sr)/(µW/cm^2)].

The remaining methods were examined using a well plate with Rhodamine B in water, Ringer's plus Dextran, and Ringer's plus Dextran and BSA in rows A, C, and E, respectively. Following are images of different methods and a short discussion of each.

Method 002

Figures 9, 10, and 11 show Method 002 applied to Rhodamine B at an exposure time of 1 second, 5 seconds, and 30 seconds, respectively. Method 2 at an exposure of 5 seconds was determined to be the best option for Method 002. There is less background "noise" at an

exposure of 5 seconds than at an exposure of 1 second. An exposure of 30 seconds causes the image to become over-exposed.

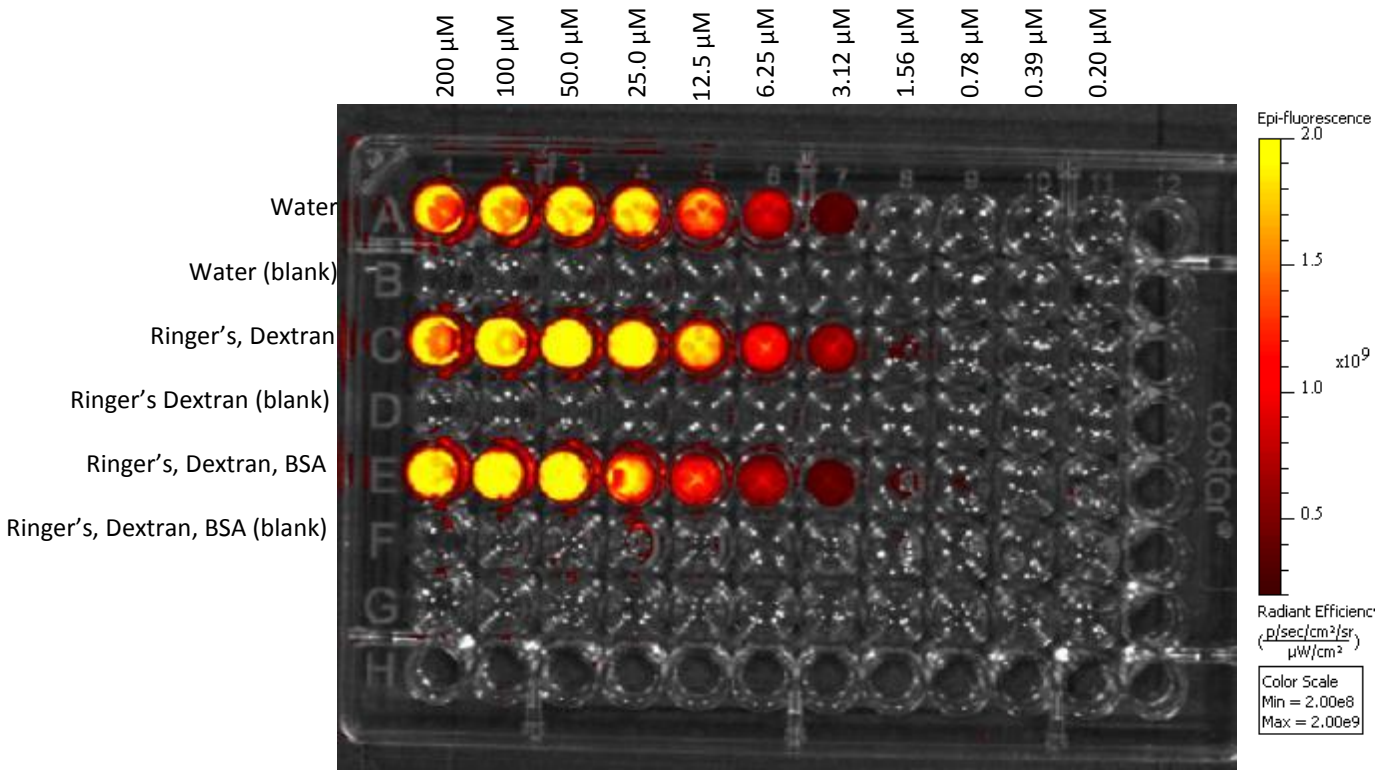

Figure 9. Well plate imaged with Rhodamine B in water, Ringer's and 6% Dextran, and Ringer's, 6% Dextran 500, and 0.1% BSA in rows A, C, and E respectively with an exposure time of 1 second and an f/stop of 2. Starting solution in column 1 is 200 µM Rhodamine B. The solution was serial diluted down each row.

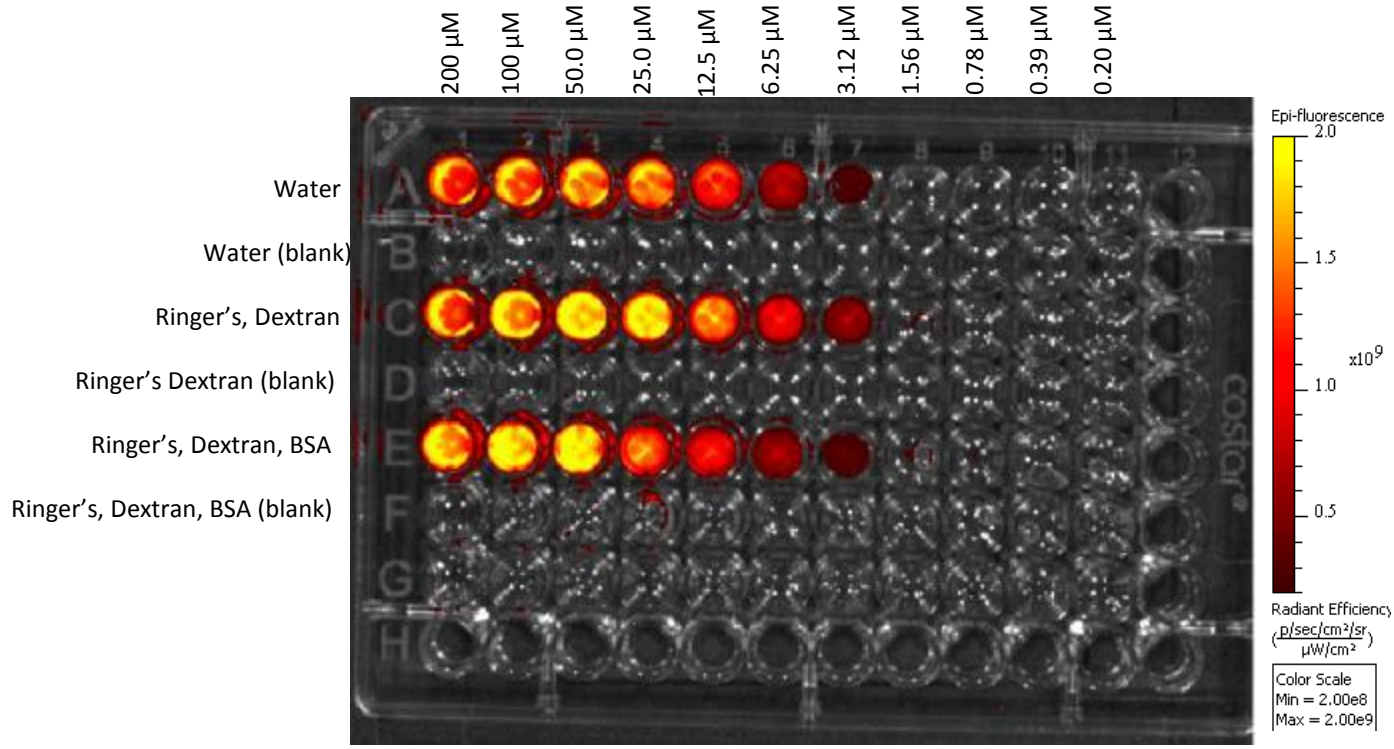

Figure 10. Well plate imaged with Rhodamine B in water, Ringer's and 6% Dextran, and Ringer's, 6% Dextran 500, and 0.1% BSA in rows A, C, and E respectively with an exposure time of 5 seconds and an f/stop of 2. Starting solution in column 1 is 200 µM Rhodamine B. The solution was serial diluted down each row.

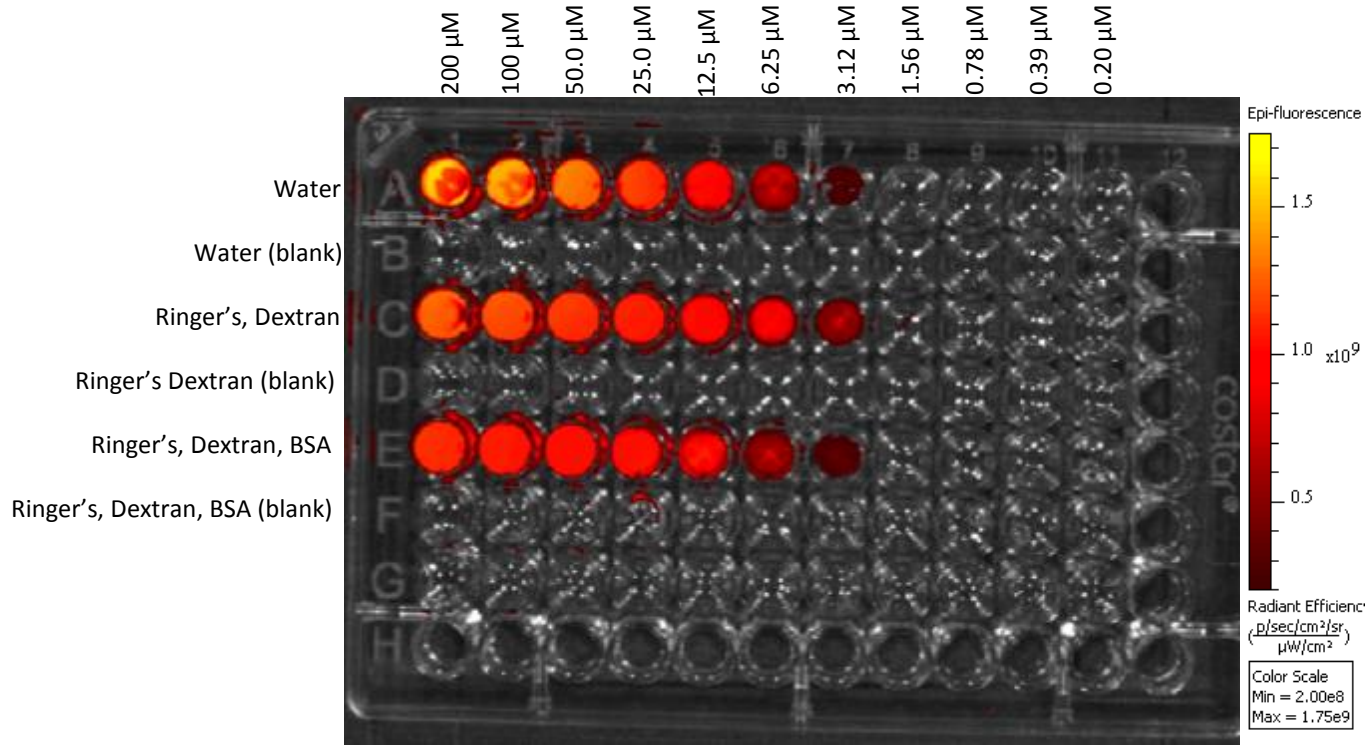

Figure 11. Well plate imaged with Rhodamine B in water, Ringer's and 6% Dextran, and Ringer's, 6% Dextran 500, and 0.1% BSA in rows A, C, and E respectively with an exposure time of 30 seconds and an f/stop of 2. Starting solution in column 1 is 200 µM Rhodamine B. The solution was serial diluted down each row.

Method 003 is the same as Method 002 except with a medium binning instead of a small binning. The medium binning provided the same amount of fluorescent information, but the small binning provided an image with better spatial resolution at the FOV used.

Method 004

Figure 12 shows Rhodamine B imaged using Method 004. An f/stop of 16 was used for Method 004 as opposed to the f/stop of 2 that was used in Method 002. The f/stop changes the amount of light that enters the camera. Smaller f/stops allow more light to enter the cameral lens than larger f/stops. The larger f/stop decreased the amount of "noise" in the image, but now there isn't any fluoresence showing in column 7 and very little in column 6. The smaller f/stop clearly showed fluoresence in these columns.

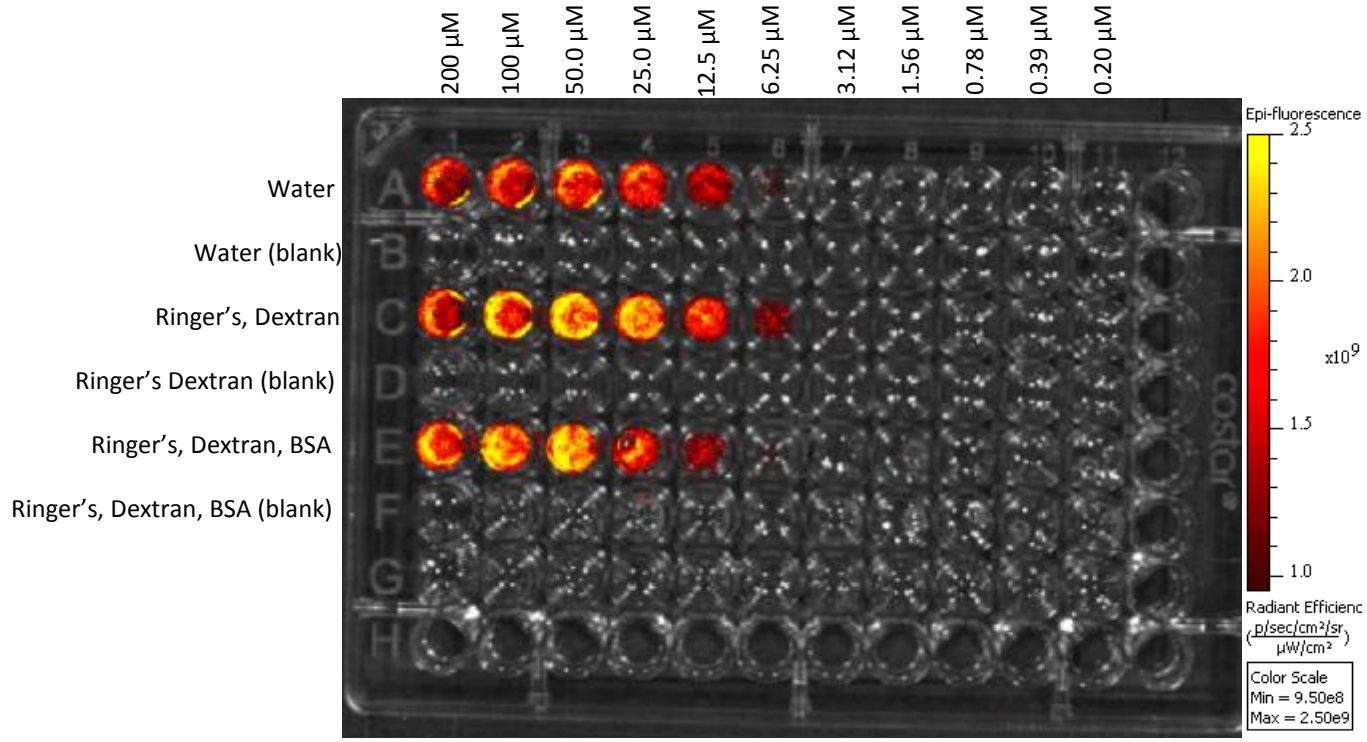

Figure 12. Well plate imaged with Rhodamine B in water, Ringer's and 6% Dextran, and Ringer's, 6% Dextran 500, and 0.1% BSA in rows A, C, and E respectively with an exposure time of 1 second and an f/stop of 16. Starting solution in column 1 is 200 µM Rhodamine B. The solution was serial diluted down each row.

Method 006

Method 006 has an f/stop of 4. Figures 13, 14, and 15 were taken using the settings of Method 006 at exposures of 1 second, 5 seconds, and 30 seconds, respectively. The 5 second and 30 second exposures both show fluorescence in the 7th column which is consistent with the settings of Method 002. At an exposure of only 1 second however, there is little fluorescence in this column.

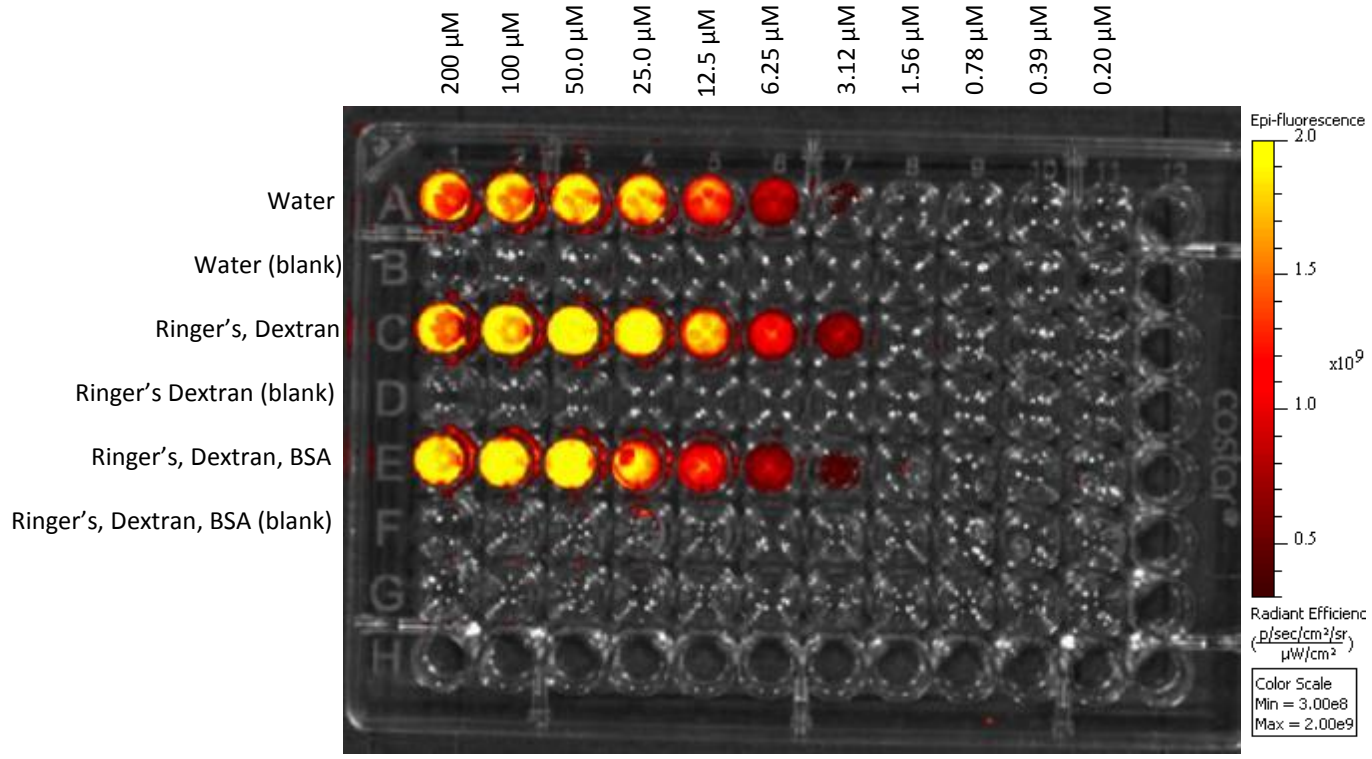

Figure 13. Well plate imaged with Rhodamine B in water, Ringer's and 6% Dextran, and Ringer's, 6% Dextran 500, and 0.1% BSA in rows A, C, and E respectively with an exposure time of 1 second and an f/stop of 4. Starting solution in column 1 is 200 µM Rhodamine B. The solution was serial diluted down each row.

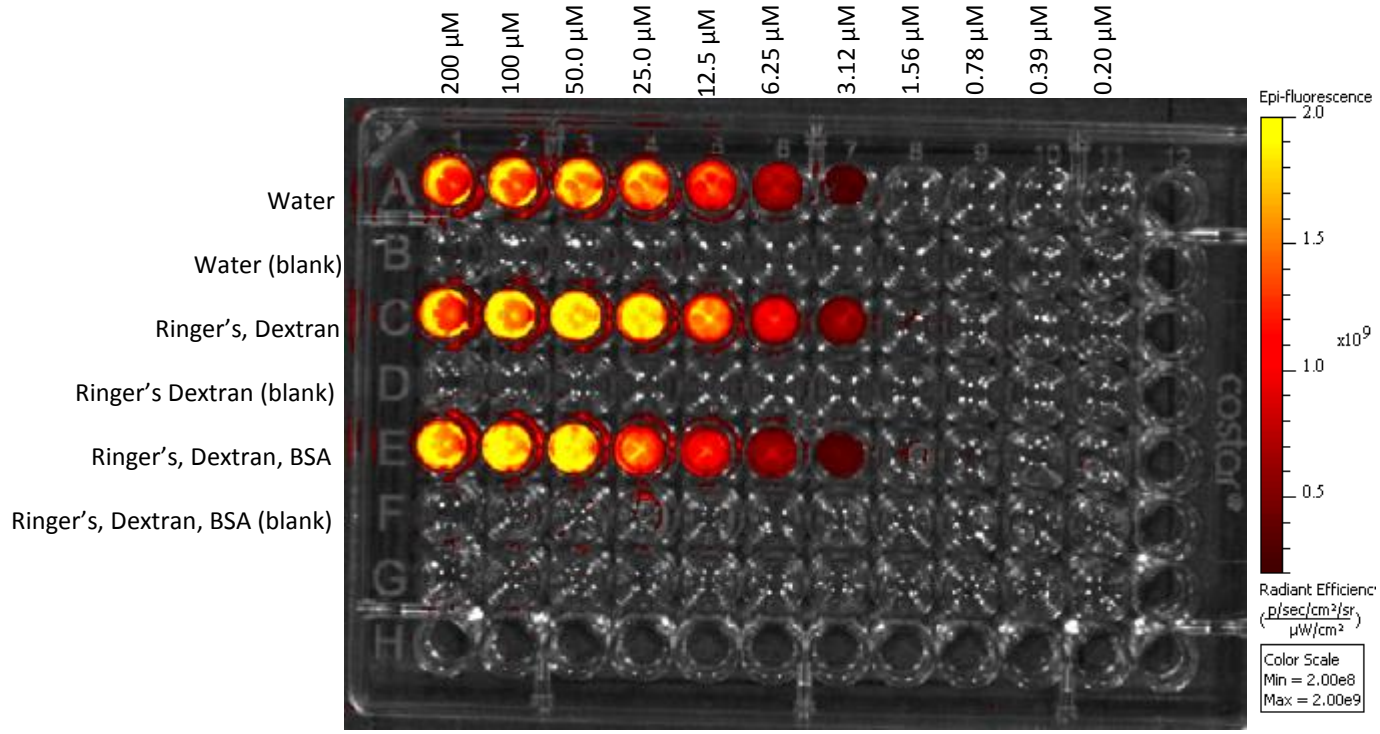

Figure 14. Well plate imaged with Rhodamine B in water, Ringer's and 6% Dextran, and Ringer's, 6% Dextran 500, and 0.1% BSA in rows A, C, and E respectively with an exposure time of 5 seconds and an f/stop of 4. Starting solution in column 1 is 200 µM Rhodamine B. The solution was serial diluted down each row.

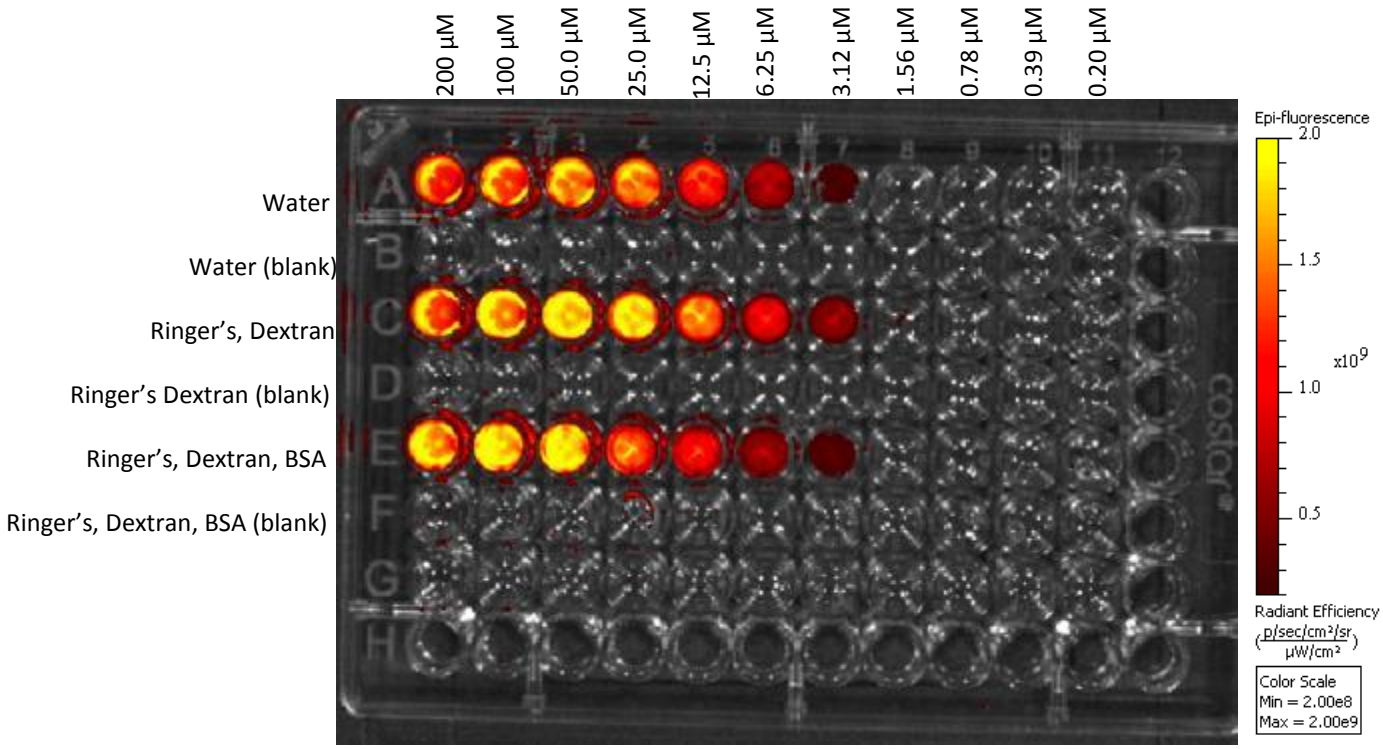

Figure 15. Well plate imaged with Rhodamine B in water, Ringer's and 6% Dextran, and Ringer's, 6% Dextran 500, and 0.1% BSA in rows A, C, and E respectively with an exposure time of 30 seconds and an f/stop of 4. Starting solution in column 1 is 200 µM Rhodamine B. The solution was serial diluted down each row.

Method 007

Figure 16 displays Rhodamine B imaged under the settings of Method 7. The f/stop used in this method (f/stop 8) is less than that of Method 004 (f/stop 16), but greater than that of Method 006 (f/stop 4). The image contains quite a bit of background.

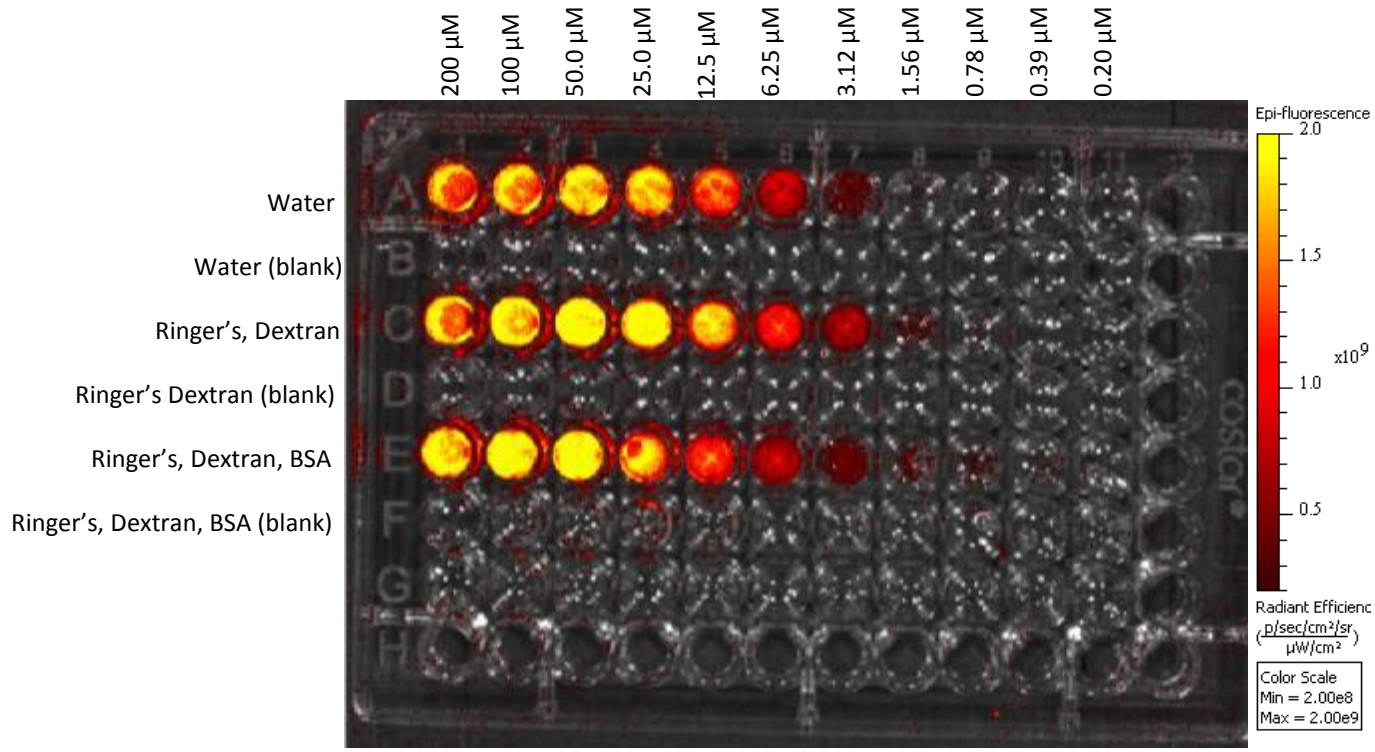

Figure 16. Well plate imaged with Rhodamine B in water, Ringer's and 6% Dextran, and Ringer's, 6% Dextran 500, and 0.1% BSA in rows A, C, and E respectively with an exposure time of 1 second and an f/stop of 8. Starting solution in column 1 is 200 µM Rhodamine B. The solution was serial diluted down each row.

Based on the differences in clarity of images between Methods 002 and 003, it was decided that the smaller binning was better than the medium binning. The spatial resolution of Method 002 is higher than Method 003 due to the smaller binning, giving the appearance of higher clarity in images taken with Method 002. The images appear to better exhibit the fluorescence data at the lower f/stops of 2 and 4. These f/stops provide somewhat cleaner fluorescence images. The exposure times presented for Methods 002 and 006 suggest that an optimal exposure time is about 5 seconds. In Method 002 the 5 second exposure time reduced background "noise", but didn't seem to overexpose the image. In Method 006 the 5 second exposure provided more data than the 1 second exposure time. The images taken at a 5 second exposure time and a 30 second exposure time for Method 006 look the same, so the shorter exposure time was ideal. The images taken at a 5 second exposure time with Method 002, f/stop

2, and with Method 006, f/stop 4, appeared to give about the same fluorescent intensity. Thus the settings for Rhodamine B imaging were based off Method 002 at an exposure time of 5 seconds.

Microdialysis Sampling

Relative Recovery

Because microdialysis involves a constant flow rate, concentration equilibrium is impossible to establish, thus relative recovery data is gathered to relate information about concentrations in the extracellular fluid. *In vitro* relative recovery experiments were performed to determine the relative recovery of Rhodamine B. The relative recovery of Rhodamine B is displayed in Table 3. The average relative recovery for 312.7 μM and 31.3 μM is 82.4%±0.58 and 64.8%±3.9, respectively.

Table 3. Relative recovery of Rhodamine B. Microdialysis probes were submersed in heated (35°C) 312.7 μM and 31.3 μM Rhodamine B in Ringer's solution and perfused with a solution of Ringer's, 6% Dextran, and 0.1% BSA.

Initial Concentration (μM)	Sample	Absorbance	Concentration (μM)	% Recovery
312.7	1	1.59	255.36	81.66
	2	1.61	257.56	82.37
	3	1.61	258.15	82.56
	4	1.62	259.76	83.07
31.3	1	0.14	19.99	63.85
	2	0.15	20.48	65.43
	3	0.15	20.34	64.98
	4	0.13	18.58	59.35
	5	0.16	21.96	70.15

In Vitro *Microdialysis*

A diffusion profile of Rhodamine B can be clearly detected via fluorescence imaging of the microdialysis process. Figure 17 shows the development of a diffusion profile surrounding a probe in agar as a function of time. Images were taken every 5 minutes for 3 hours. The top and

bottom phantom in each image is perfused with 20 μM and 200 μM Rhodamine, respectively. For the 200 μM infusion, the profile is clearly visible after only 10 minutes of microdialysis sampling, and the 20 μM concentration is not visible until around 40 minutes. The 20 μM was tested by itself in the IVIS system, and fluorescence is also visible starting at about 10 minutes, but it doesn't develop a profile similar to the 200 μM at 10 minutes until about 40 minutes of perfusion. See Figure 18. The IVIS machine automatically scales each image, but the images can be manually scaled. Images that were taken towards the beginning of the process can be scaled in such a way that the lower concentration becomes visible. Doing this however, causes a lot of background "noise" to appear around the phantom with the higher concentration (displayed in Figure 19), thus the images were scaled to reduce background around the phantom perfused with the 200 μM Rhodamine B.

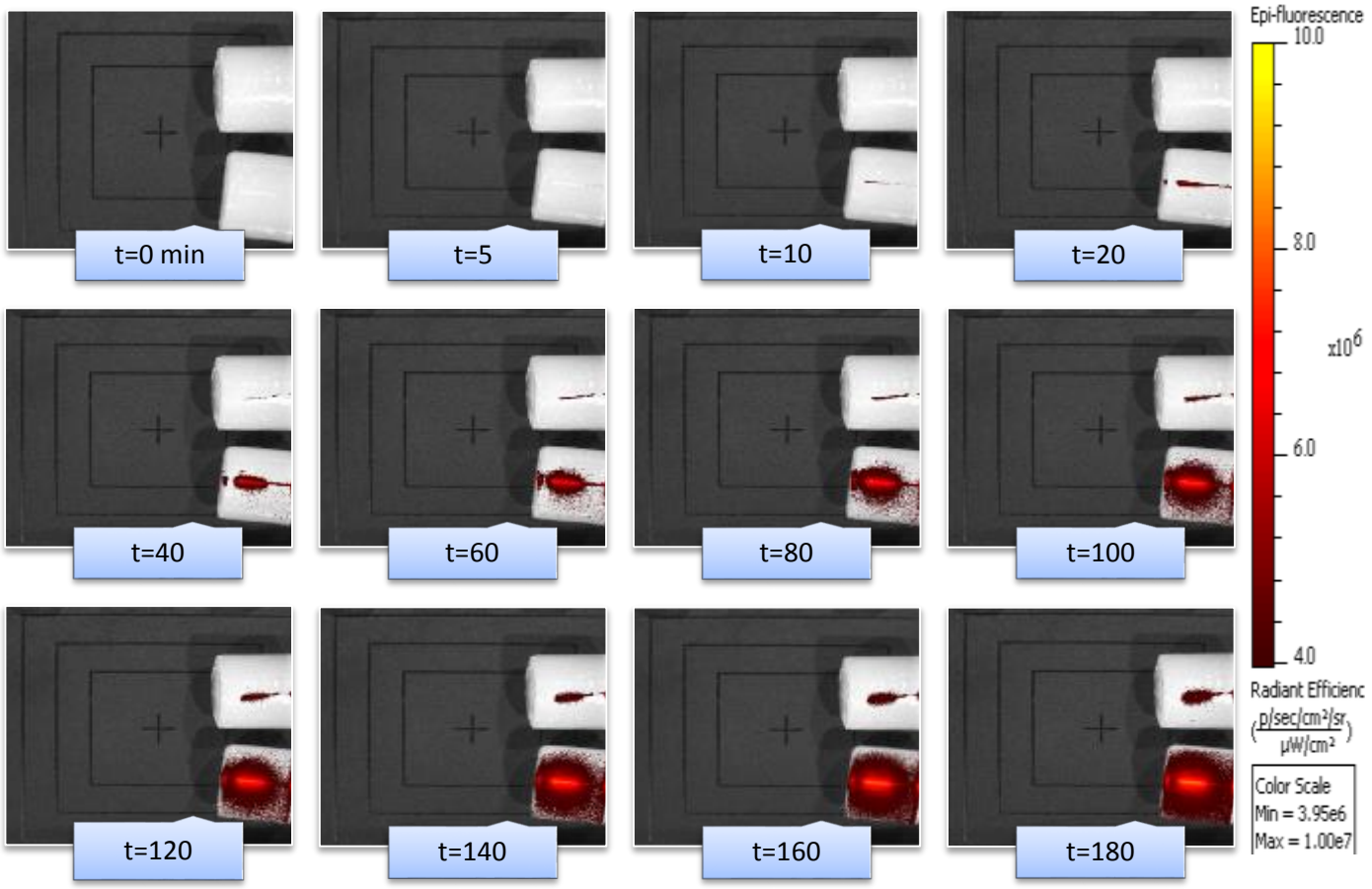

Figure 17. Rhodamine B microdialysis diffusion profile over time in agar phantoms. The top and bottom phantom in each image is perfused with 20 µM and 200 µM, respectively.

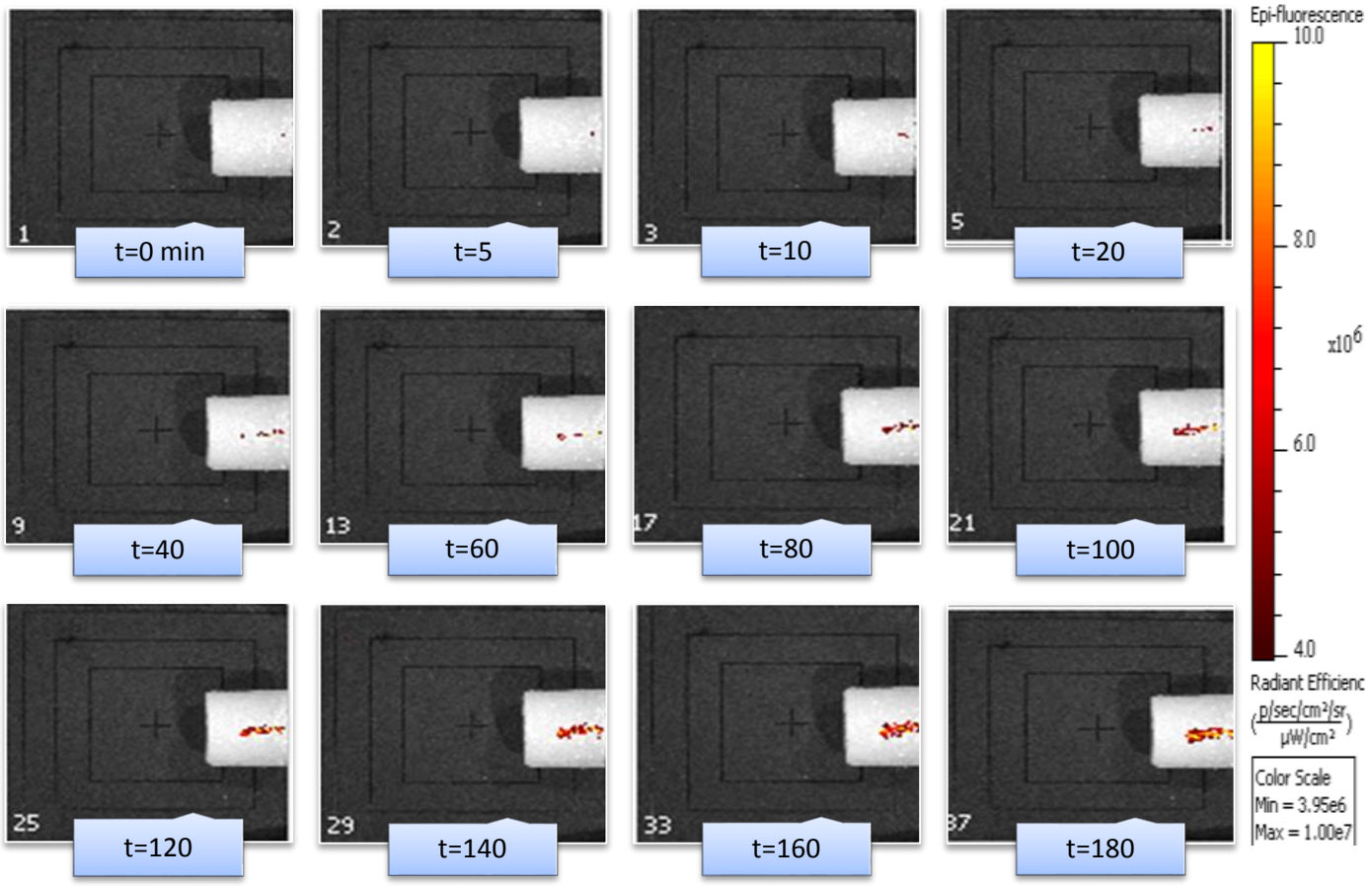

Figure 18. 20 µM Rhodamine B microdialysis diffusion profile over time in agar phantoms.

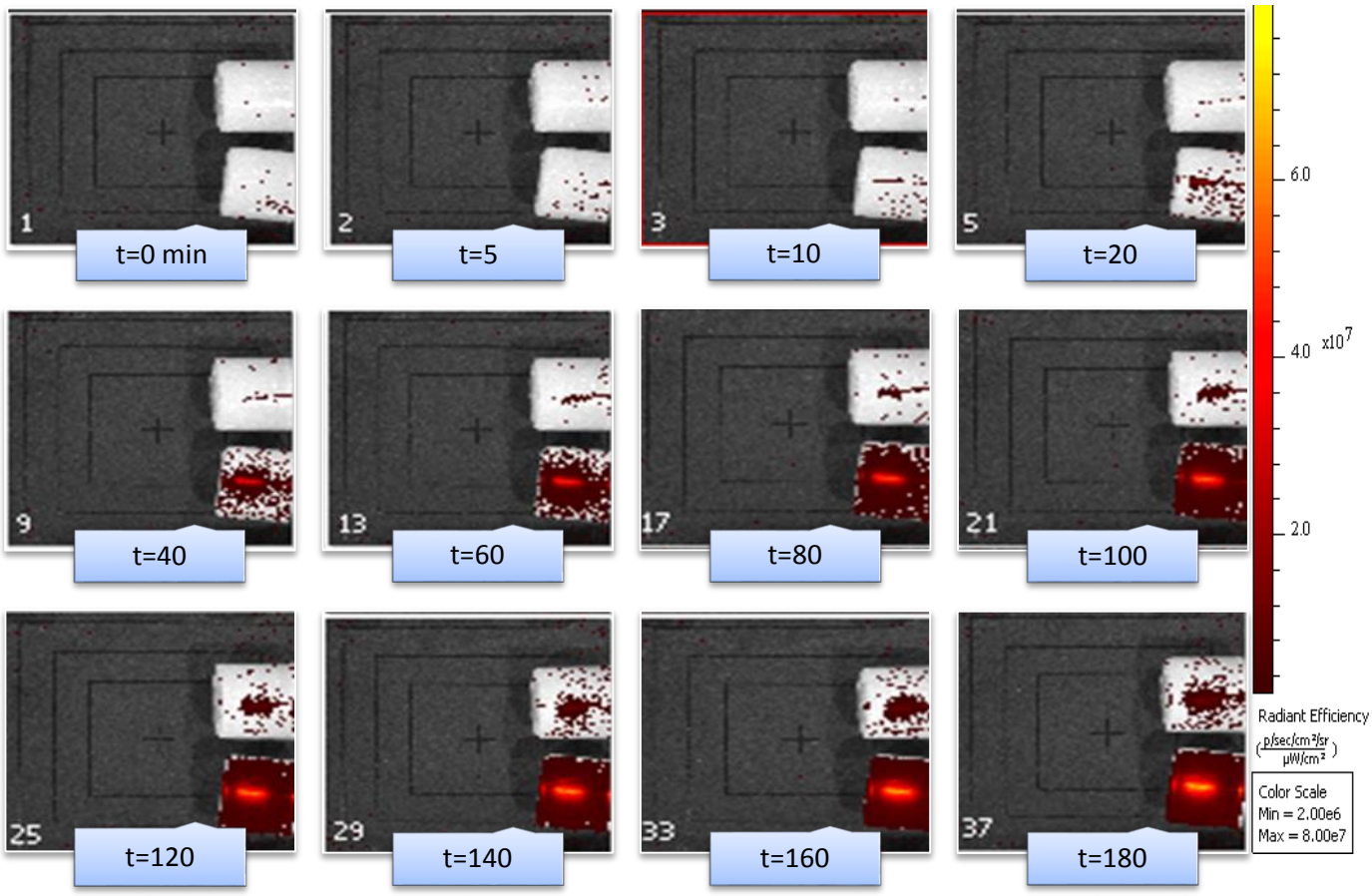

Figure 19. Scale was changed to bring out the profile of the lower concentration at an earlier time. You can see the profile starting at about 20 minutes, but it creates a lot of "noise". This is evident by the fluorescent signals showing up far away from where the dye could be.

Starting at time t = 40 minutes, there is some fluorescence on the phantom, but too far from the probe to be dye. This is background "noise" that cannot be completely removed without affecting the diffusion profile around the probe. To obtain data when this "noise" is present, regions of interest (ROIs) can be selected. ROIs provide fluorescence data (radiant efficiency or counts) within the region selected. ROIs can be selected automatically or manually. By manually selecting a ROI, the background "noise" on the phantom can be ignored and the fluorescence data around the probe can be reported.

Reproducibility of *In Vitro* Studies

The *in vitro* studies were repeated to determine the reproducibility of their results. As shown in the following figures, the process is very reproducible; the experiments all returned similar images.

Figure 20. Run 1. Time course infusion of Rhodamine B for 3 hours.

Figure 21. Run 2. Time course infusion of Rhodamine B for 3 hours.

Figure 22. Run 3. Time course infusion of Rhodamine B for 3 hours.

Figure 23. Run 4. Time course infusion of Rhodamine B for 3 hours.

Figure 24. Run 5. Time course infusion of Rhodamine B for 3 hours.

Figure 25. Run 6. Time course infusion of Rhodamine B for 3 hours.

In Vivo Studies

A naïve rat was imaged under the same imaging settings for the Rhodamine B *in vitro* studies. As Figure 26 reveals, there is a considerable amount of natural fluorescence from the animal at the appropriate wavelengths for imaging the infusion of Rhodamine B. This "auto-fluorescence" of tissue and biosubstrates creates a significant problem in rendering background subtraction of fluorescence images of the infusion process impossible and *in vivo* imaging at wavelengths necessary for Rhodamine B impossible.

An *in vivo* imaging protocol by Perkin Elmer stated that the rat's hair can block, absorb, and scatter light due to a high chlorophyll diet.[18] This problem also occurs in the NIR range of light because chlorophyll tends to "auto-fluoresce" at around 700 nm. Recommendations made

to adjust for this include shaving the area of the rat to be imaged and changing the rat's diet to one consisting of a low chlorophyll concentration about two weeks before imaging.

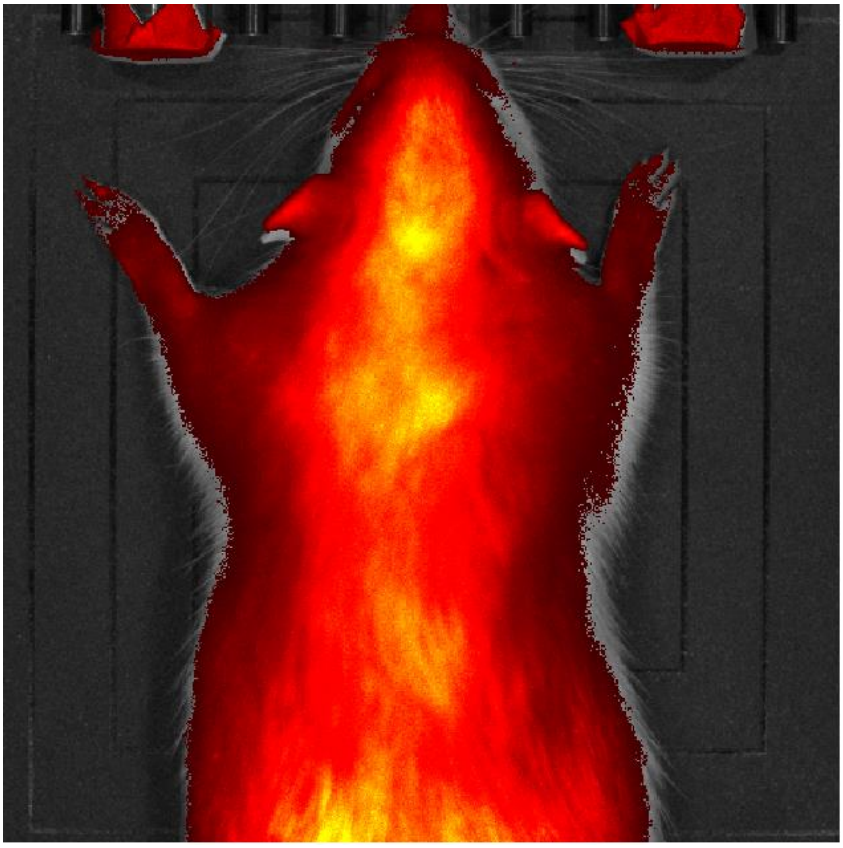

Figure 26. Naïve rat imaged with the following settings: excitation/emission filters – 535/Cy5.5, small binning, f/stop 2, and 1 s exposure time.

5. Conclusion

The IR-820 dye is unpredictable during *in vitro* studies. It is recommended that more the behavior of IR-820 be studied further before using it in conjunction with the method proposed in this paper. It is possible that dissolving IR-820 in an organic solvent will correct the problems we had, however that was not tested here.

In vitro infusion of Rhodamine B into agarose gels clearly reveals the diffusion of dye throughout the gel and an increase in fluorescence intensity surrounding the probe over time. Relative recovery of Rhodamine B shows increased recovery over the course of the experiment.

These findings are foundational for future *in vitro* work and mathematical modeling, as well as being a springboard for *in vivo* experiments. These studies strongly suggest the possibility of combining *in vivo* microdialysis sampling with *in vivo* fluorescence imaging for different biomedical related research.

Future goals should include using a near-infrared (NIR) dye that is more suitable for *in vivo* work and monitoring the diffusion profile of elastase. Modeling for the new NIR dye *in vitro* and *in vivo* diffusion profiles should be developed by fluorescence imaging of the dye in microdialysis via a live imaging instrument. The same imaging technique used for Rhodamine B can be applied to the NIR dye along with the appropriate excitation/emission filters. Using an iterative approach, the dye should be infused at varying concentrations in agarose gels via microdialysis to determine a concentration that is sufficient to provide a signal in the instrument. The temporal resolution of the instrument, 0.5 s, can be optimized as needed to obtain appropriate diffusion profiles. It is suggested that ROIs be determined for the diffusion profiles of the gels, and an *in vitro* standard curve produced. An *in vitro* study of elastase can then be conducted by applying the mentioned techniques for the NIR dye studies using phantoms with porcine elastase (a mimic for MMP-12).

6. References

1. Wang, Y.; Zagorevski, D. V.; Stenken, J. A., In situ and multisubstrate detection of elastase enzymatic activity external to microdialysis sampling probes using LC-ESI-MS. *Anal. Chem.* 2008, 80, 2050-7.
2. Wang, Y.; Zagorevski, D. V.; Lennartz, M. R.; Loegering, D. J.; Stenken, J. A., Detection of in vivo matrix metalloproteinase activity using microdialysis sampling and liquid chromatography/mass spectrometry. *Anal. Chem.* 2009, 81, 9961-71.
3. Steuerwald, A. J.; Villeneuve, J. D.; Sun, L.; Stenken, J. A., In vitro characterization of an in situ microdialysis sampling assay for elastase activity detection. *J. Pharm. Biomed. Anal.* 2006, 40, 1041-7.
4. Stenken, J. A., Methods and issues in microdialysis calibration. *Anal. Chim. Acta* 1999, 379, 337-357.

5. Cook, J. R.; Bouchar, R. R.; Emelianov, S. Y., Tissue-mimicking phantoms for photoacoustic and ultrasonic imaging. *Biomedical Optics Express* 2011, 2, 14.
6. Robinson, T. E.; Justice, J., Jr.; Editors, *Microdialysis in the Neurosciences*. Elsevier Science Ltd.: Amsterdam, 1991; p 450.
7. Westerink, B. H. C.; Cremers, T. I. F. H., *Handbook of microdialysis : methods, applications, and perspectives*. 1st ed.; Elsevier/Academic Press: Amsterdam ; Boston, 2007.
8. de Lange, E. C. M., *Microdialysis in Drug Development*. American Association of Pharmaceutical Scientists: Leiden, Netherlands, 2013; p 338.
9. Cussler, E. L., *Diffusion, mass transfer in fluid systems, Third Edition*. Cambridge University Press: Cambridge Cambridgeshire ; New York, 2009.
10. Nolting, D. D.; Gore, J. C.; Pham, W., Near-Infrared Dyes: Probe Development and Applications in Optical Molecular Imaging. *Curr. Org. Synth.* 2011, 8, 521-534.
11. Rao, J.; Dragulescu-Andrasi, A.; Yao, H., Fluorescence imaging in vivo: recent advances. *Curr. Opin. Biotechnol.* 2007, 18, 17-25.
12. Living Image Software: User's Manual. Caliper Life Sciences: Hopkinton, MA, 2011; p. 335. http://www2.udel.edu/ctcr/sites/udel.edu.ctcr/files/Living_Image_4-2_User_Guide.pdf (accessed 4/8/2014).
13. CCD Binning. http://www.andor.com/learning-academy/ccd-binning-what-does-binning-mean (accessed April 19).
14. Integrating Gold Standard Bioluminescence, Fluorescence and X-Ray In Vivo Technologies. https://www.thermofisher.com.au/Uploads/file/Scientific/Life-Science-Research-Technologies/In-Vivo-Imaging/In-vivo-Imaging-Systems/IVIS_Lumina_XR_Series_III.pdf (accessed April 8).
15. Material Safety Data Sheet. 4.2 ed.; Sigma-Aldrich: 2014.
16. Prajapati, S. I.; Martinez, C. O.; Bahadur, A. N.; Wu, I. Q.; Zheng, W.; Lechleiter, J. D.; McManus, L. M.; Chisholm, G. B.; Michalek, J. E.; Shireman, P. K.; Keller, C., Near-infrared imaging of injured tissue in living subjects using IR-820. *Mol Imaging* 2009, 8, 45-54.
17. Rhodamine B. http://www.sigmaaldrich.com/catalog/product/sigma/r6626?lang=en&region=US (accessed 19).
18. *In vivo* Imaging Protocol. Elmer, P., Ed. PerkinElmer, Inc.: Waltham, MA, 2010.